

-A134 348

RIA-83-U490

TECHNICAL
LIBRARY

ADA 134348

MEMORANDUM REPORT ARBRL-MR-03313

(Supersedes IMR No. 753)

ADVANCED TECHNIQUES FOR ANALYZING
DYNAMIC FRAGMENTS

John A. Zook
Donald F. Merritt

October 1983



US ARMY ARMAMENT RESEARCH AND DEVELOPMENT CENTER
BALLISTIC RESEARCH LABORATORY
ABERDEEN PROVING GROUND, MARYLAND

Approved for public release; distribution unlimited.

Destroy this report when it is no longer needed.
Do not return it to the originator.

Additional copies of this report may be obtained
from the National Technical Information Service,
U. S. Department of Commerce, Springfield, Virginia
22161.

The findings in this report are not to be construed as
an official Department of the Army position, unless
so designated by other authorized documents.

*The use of trade names or manufacturers' names in this report
does not constitute endorsement of any commercial product.*

UNCLASSIFIED

SECURITY CLASSIFICATION OF THIS PAGE (When Data Entered)

REPORT DOCUMENTATION PAGE		READ INSTRUCTIONS BEFORE COMPLETING FORM
1. REPORT NUMBER MEMORANDUM REPORT ARBRL-MR-03313	2. GOVT ACCESSION NO. AD-A 134 348	3. RECIPIENT'S CATALOG NUMBER
4. TITLE (and Subtitle) ADVANCED TECHNIQUES FOR ANALYZING DYNAMIC FRAGMENTS		5. TYPE OF REPORT & PERIOD COVERED FINAL
		6. PERFORMING ORG. REPORT NUMBER
7. AUTHOR(s) John A. Zook and Donald F. Merritt		8. CONTRACT OR GRANT NUMBER(s)
9. PERFORMING ORGANIZATION NAME AND ADDRESS US Army Ballistic Research Laboratory, ARDC ATTN: DRSMC-BLT(A) Aberdeen Proving Ground, MD 21005		10. PROGRAM ELEMENT, PROJECT, TASK AREA & WORK UNIT NUMBERS RDT&E 1L162618AH80
11. CONTROLLING OFFICE NAME AND ADDRESS US Army AMCCOM, ARDC Ballistic Research Laboratory, ATTN:DRSMC-BLA-S(A) Aberdeen Proving Ground, MD 21005		12. REPORT DATE October 1983
14. MONITORING AGENCY NAME & ADDRESS (if different from Controlling Office)		13. NUMBER OF PAGES 34
		15. SECURITY CLASS. (of this report) Unclassified
		15a. DECLASSIFICATION/DOWNGRADING SCHEDULE
16. DISTRIBUTION STATEMENT (of this Report) Distribution unlimited, approved for public release.		
17. DISTRIBUTION STATEMENT (of the abstract entered in Block 20, if different from Report)		
18. SUPPLEMENTARY NOTES This report supersedes LMR No. 753.		
19. KEY WORDS (Continue on reverse side if necessary and identify by block number) Data Acquisition X-ray System Fragments Mass Velocity		
20. ABSTRACT (Continue on reverse side if necessary and identify by block number) This report presents three different levels of analytic techniques for determining mass and velocity of dynamic fragments (fragments in motion). The first level describes recent advancements for analyzing images on flash radiographs. This advancement has reduced the amount of physical labor and inaccuracies, but the procedure can still be made less tedious by introducing the system which constitutes the second level. This second level consists of a proposed technique for eliminating the need to digitize the film manually. The third level		

UNCLASSIFIED

SECURITY CLASSIFICATION OF THIS PAGE(When Data Entered)

is the development of the Automatic Data Acquisition System (ADAS), which is the ultimate in automatic recording of dynamic fragment images. This system will minimize the tedious handwork for the analyst and will significantly increase the accuracy of the results. It may also be found that the ADAS will be useful for studying other physical phenomena such as shaped charge jet and self-forging fragment formation.

UNCLASSIFIED

SECURITY CLASSIFICATION OF THIS PAGE(When Data Entered)

TABLE OF CONTENTS

	<u>Page</u>
LIST OF FIGURES.....	5
I INTRODUCTION.....	7
II. ANALYSIS OF FRAGMENT IMAGES.....	7
II.1 SCALING THE FILM COORDINATE POINTS TO THE SPATIAL CO- ORDINATES.....	8
II.2 MATCHING ORTHOGONAL FILM IMAGES AND CALCULATING FRAGMENT MASS.....	14
II.3 A TEST OF THE METHODOLOGY FOR MATCHING IMAGES AND THE DETERMINATION OF THE FRACTIONAL VALUE q	20
II.4 ESTIMATING FRAGMENT VELOCITY BASED ON ORTHOGONAL FILM IMAGES.....	24
III. AUTOMATING THE FILM DIGITIZATION PROCESS.....	27
IV. THE AUTOMATIC DATA ACQUISITION SYSTEM (ADAS).....	28
V. SUMMARY AND CONCLUSIONS.....	32
ACKNOWLEDGEMENTS.....	32
DISTRIBUTION LIST.....	33

LIST OF FIGURES

<u>Number</u>		<u>Page</u>
1	Geometric Relationship Of Orthogonal X-Ray Tubes To The Film Planes.....	9
2	Expanded View Of The Geometry Close To The Origin.....	11
3	View Of The X-Y Plane With $Z=0$	12
4	Representation Of The Image By Interconnecting Straight Line Segments.....	17
5	Representing The Image By A Rectangle Of Equivalent Area And Indicating The K Factor Associated With Each Point...	19
6	Block Diagram Of The ADAS.....	29
7	Schematic Representation Of A Vidicon Tube.....	30

I. INTRODUCTION

Terminal ballisticians have the requirement for knowing the mass and velocity of fragments generated by munition impacts on armor targets. In the past, a great deal of human effort has been expended in order to acquire this information and often the accuracy of the the data is poor. For example, the fragments produced behind target plates have been recovered by stopping them in celotex and the masses of the fragments and their direction of travel can be determined quite accurately after a lot of tedious work, but the speed of the fragments can only be estimated.

An alternative method to capturing the fragments in celotex is to capture images of the fragments in flight on film by pulsing orthogonal X-ray tubes at known times. Again, a great deal of human effort is required to analyze the film, often with unsatisfactory results. The problem is that it is difficult to correlate orthogonal images of fragments (required in order to determine fragment mass) and even more difficult to identify multiple fragment images in the same view produced by a multiframe sequence which is needed to obtain accurate fragment velocities.

The difficulties associated with fragment data acquisition and analysis can now be alleviated by recent advancements in computer and video technology. It is now feasible to automate the data acquisition and analysis system so that the amount of human effort will be greatly reduced and the accuracy and speed in the analysis substantially enhanced. This report describes recent advancements in fragment image analysis and presents the technical basis for a proposed Automatic Data Acquisition System (ADAS).

II. ANALYSIS OF FRAGMENT IMAGES

The mathematical procedure for analyzing the fragment image data in the ADAS will be essentially the same as that used for the film image data. However, in the ADAS, the images will be recorded electronically and the analysis performed automatically. In order to show the feasibility of the ADAS, it is first necessary to discuss the procedure for calculating the mass and velocity of the fragments from the film data. The basis for this analytical procedure has been reported previously,¹ but some modifications which constitute improvements in the technique are presented in this section.

¹A. L. Arbuckle, E. L. Herr, A. J. Ricchiazzi, "A Computerized Method of Obtaining Behind-the-Target Data From Orthogonal Flash Radiographs," BRL MR 2264, January 1973 (AD 908362L).

II.1 SCALING THE FILM COORDINATE POINTS TO THE SPATIAL COORDINATES

The following analysis is based on the typical X-ray system² used at the BRL. The geometric relationship of the orthogonal X-ray tubes to the film is depicted in Figure 1. As shown, the origin of the coordinate system is defined to be the intersection of the two film planes (the X-Z plane and Y-Z plane) with the X-Y plane. The X-Y plane is formed by the centerlines of the orthogonal X-ray tubes. The centerline of the horizontal tube is oriented parallel to the X axis with the tube facing the Y-Z plane (vertical film plane) and is a distance Y_{ff} above the X axis. The forward tip of the horizontal tube is a distance X_{hf} from the Y-Z plane. The centerline of the vertical tube is oriented parallel to the Y axis with the tube facing the X-Z plane (horizontal film plane) and is a distance X_{ff} away from the Y axis. The forward tip of the vertical tube is a distance Y_{hf} from the X-Z film plane.

Reference marks needed to analyze the image data are made on the film by fiducial wires. A fiducial wire parallel to the Z axis is located directly in front of the vertical film at a distance Y_{ff} above the Z axis. Another fiducial wire parallel to the Z axis lies directly above the horizontal film at a distance X_{ff} away from the Z axis. Fiducial wires (not visible in Figure 1) are also strung along the X axis and the Y axis. The point of intersection of each pair of fiducial wires lies on the centerline axis of the orthogonal X-ray tube which faces that point.

In order to determine the spatial coordinates (coordinates of points lying in the space directly in front of both film planes) of certain points on the fragments from corresponding points on their respective images on the orthogonal films, it is necessary to scale the film coordinates of the points on the film. (The coordinates of points located on the film surface will be referred to as film coordinates and have the same reference origin as the spatial coordinates.) The reason that the film coordinates must be scaled to the spatial coordinates is due to the fact that each X-ray tube acts as a point source of radiation. Therefore, any point in space between the tube head and the film except those points lying on the X-ray tube centerline will be nonisometrically projected onto the film. (The points that lie on the centerline are isometrically projected.) The derivation of the equations for evaluating the appropriate scaling factors to translate the film coordinates

²Chester Grabarek, Louis Herr, "X-Ray Multiflash System for Measurement of Projectile Performance at the Target," BRL TN 1634, September 1966 (AD 807619).

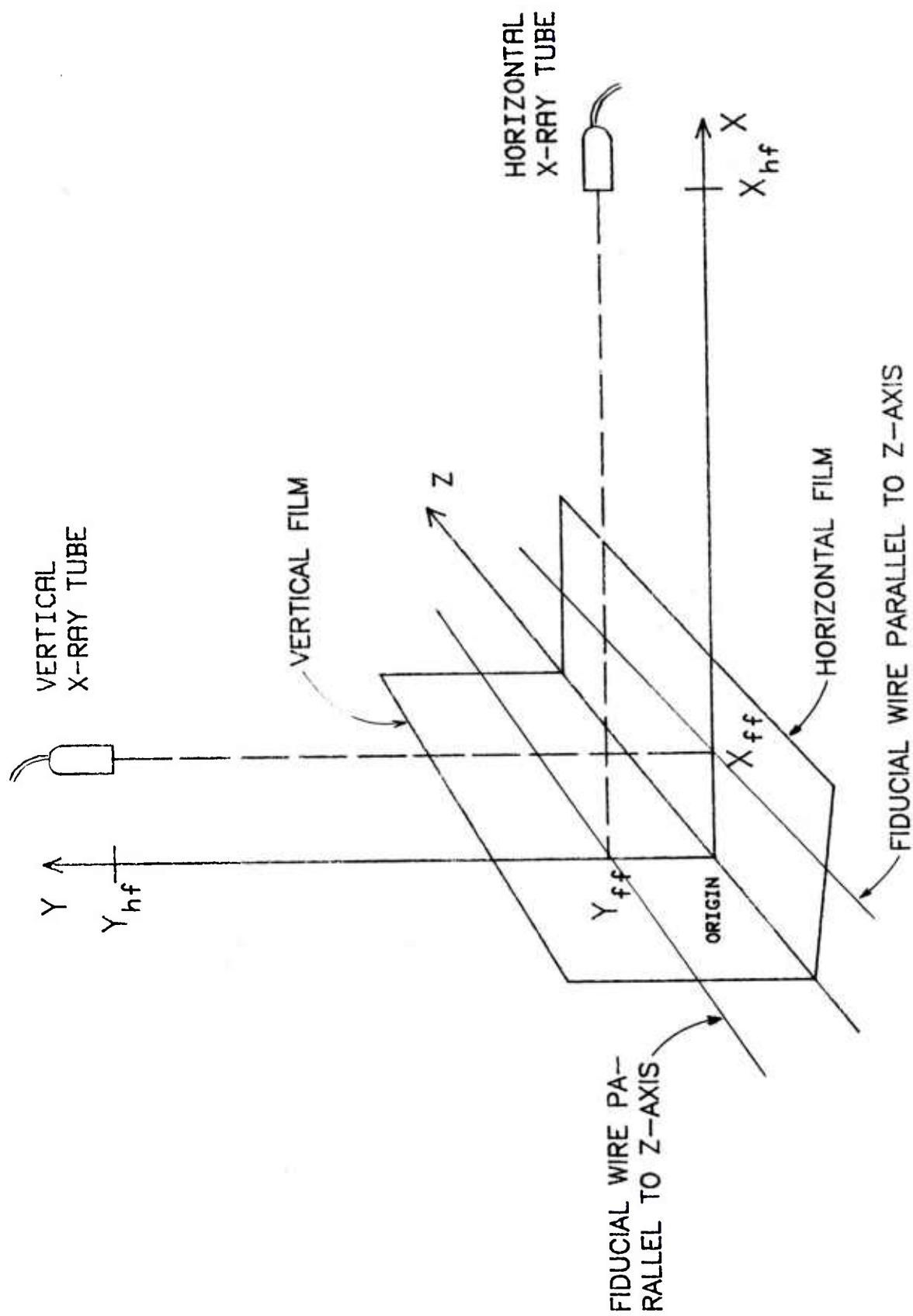


Figure 1 Geometric Relationship Of Orthogonal X-Ray Tubes To The Film Planes.

to the spatial coordinates is described in the remainder of this section.

The equations from which the scaling factors are derived result from the geometric relationship of the X-ray tubes to the film planes. Figure 2 is an expanded view of Figure 1 in the region close to the origin. Not shown is the point X_p, Y_p, Z_p in space which lies at the intersection of the lines drawn from each X-ray tube to its corresponding film image point. The coordinates of the vertical film image point are Y_1, Z_v and the coordinates of the horizontal film image point are X_1, Z_h . The following equations are derived based on the rules for similar triangles:

$$\frac{Z_v}{Y_1 - Y_{ff}} = \frac{Z_p}{Y_p - Y_{ff}} \quad (1)$$

$$\text{and} \quad \frac{Z_h}{X_{ff} - X_1} = \frac{Z_p}{X_{ff} - X_p} \quad (2)$$

Two more equations can be derived in a similar manner based on the geometry shown in Figure 3. These equations are:

$$\frac{X_{hf}}{Y_1 - Y_{ff}} = \frac{X_p}{Y_1 - Y_p} \quad (3)$$

$$\text{and} \quad \frac{Y_{hf}}{X_{ff} - X_1} = \frac{Y_p}{X_p - X_1} \quad (4)$$

From these equations, a scaling factor for each film plane can be derived. The scaling factor is defined as the value needed to scale the film Z coordinate value to the spatial Z coordinate value. Adopting the symbol used in Reference 1 for the scaling factor, the scaling factor for the vertical film plane is by definition:

$$K_v = Z_p/Z_v \quad (5)$$

The equation for calculating the value for K_v is found by solving Equations 1, 3 and 4 simultaneously. This is done by taking Equation 3, solving for X_p and substituting the result in Equation 4. The expression found by cross multiplying, expanding and solving for Y_p is then substituted into Equation 1

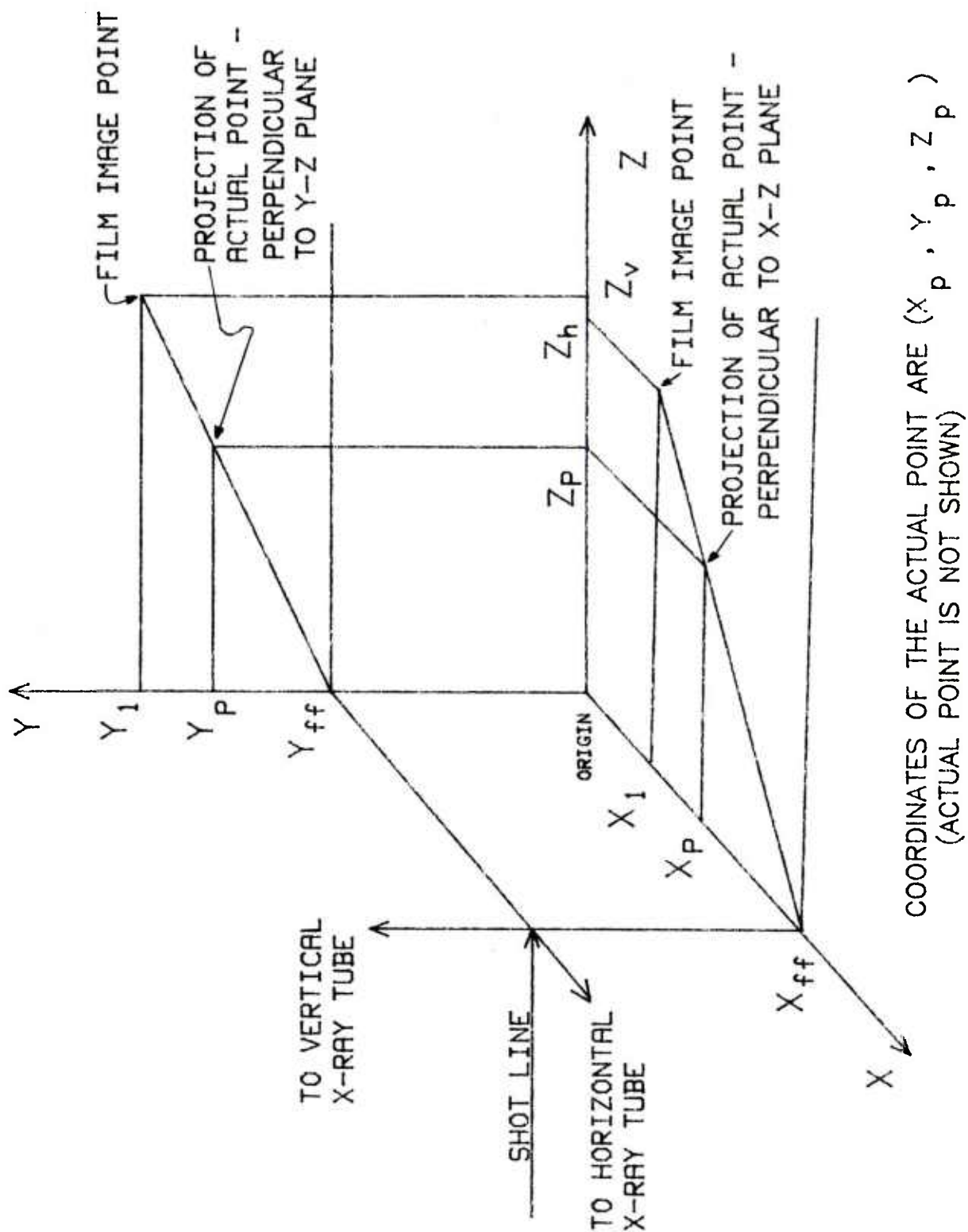


Figure 2 Expanded View Of The Geometry Close To The Origin

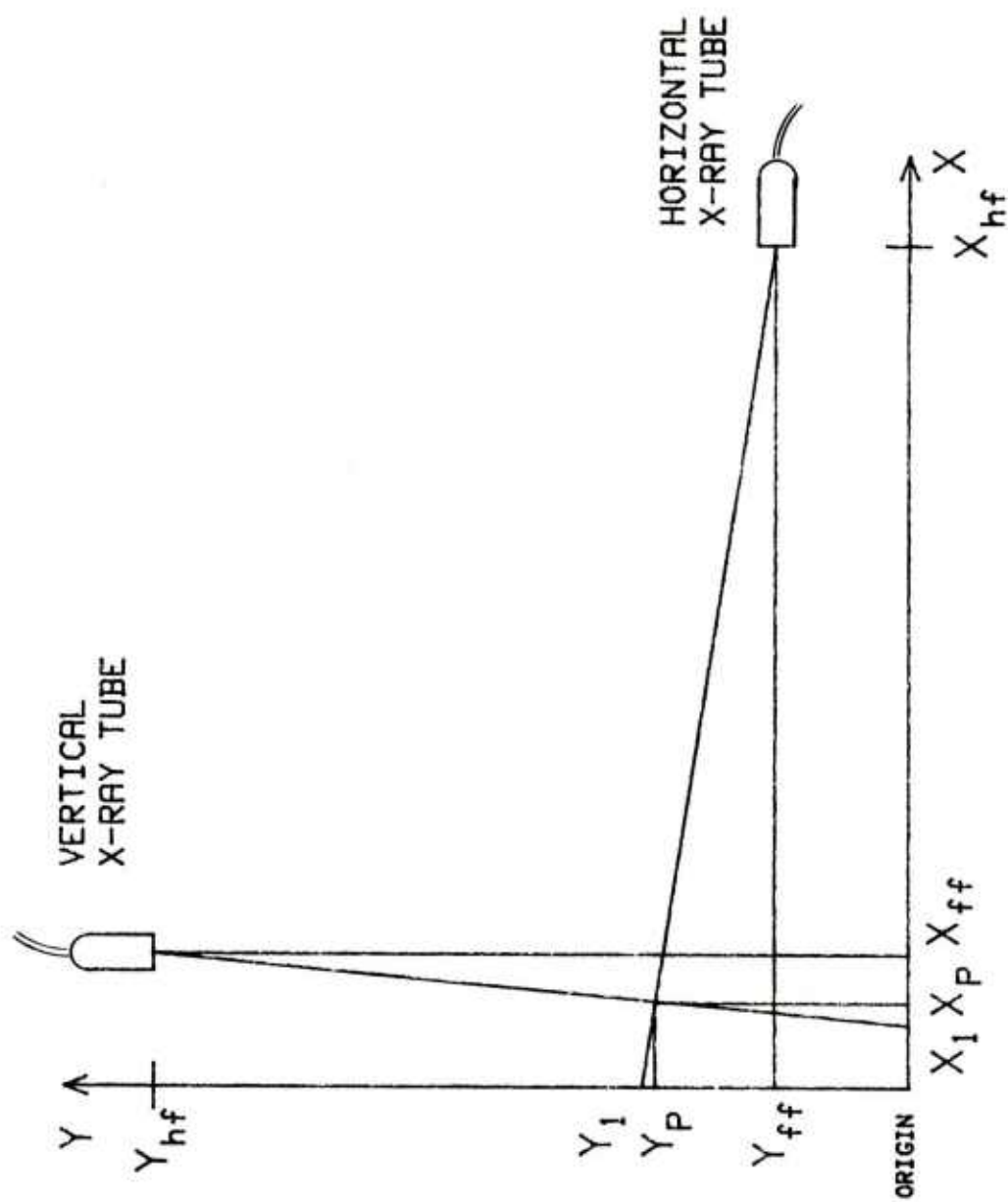


Figure 3 View Of The X-Y Plane With $Z=0$.

and rearranged in accordance with Equation 5. The result is:

$$K_v = \frac{Y_{hf}(X_{hf} - X_1) - Y_{ff}(X_{ff} - X_1)}{X_{hf}Y_{hf} + (X_{ff} - X_1)(Y_1 - Y_{ff})} . \quad (6)$$

Similarly to Equation 5, the scaling factor for the horizontal film is by definition:

$$K_h = Z_p/Z_h . \quad (7)$$

Following a similar procedure as that used to obtain Equation 6, but using Equations 2, 3, 4 and 7, will yield the following equation.

$$K_h = -\frac{X_{hf}(Y_{hf} - Y_1) + X_{ff}(Y_1 - Y_{ff})}{X_{hf}Y_{hf} + (X_{ff} - X_1)(Y_1 - Y_{ff})} . \quad (8)$$

The equations for scaling the film coordinate points to the spatial coordinate points using both K factors are derived as follows. Rearranging Equations 5 and 7 results in the equations for calculating Z_p which are:

$$Z_p = K_v Z_v \quad (9a)$$

$$\text{or} \quad Z_p = K_h Z_h . \quad (9b)$$

That is, Z_p can be calculated from the Z film coordinate value from either orthogonal film when using the appropriate K factor. By substituting Equation 9a into Equation 1 and rearranging, the equation to calculate the value for Y_p is:

$$Y_p = Y_{ff} + K_v(Y_1 - Y_{ff}) , \quad (10)$$

and, similarly, by substituting Equation 9b into Equation 2 and rearranging, the equation for calculating the value of X_p is:

$$X_p = X_{ff} - K_h(X_{ff} - X_1) . \quad (11)$$

In general, the values for K_v and K_h are not equal but there are particular spatial points for which they are equal. These points can be determined by setting Equation 6 equal to Equation 8 and solving for X_1 for a given Y_1 .

To obtain maximum accuracy in evaluating the X and the Y spatial coordinate, the respective K factor should be used. However, there are some situations in which this can not be done. For example, when the target is at an oblique angle to the vertical plane, any fragments in the region directly in front and the region directly behind the target will be masked by the image of the target plate on the horizontal film. For these fragments, the only images appearing will be on the vertical film. In such cases, an assumption must be made about determining the spatial locations of these fragments since there is insufficient information to calculate their locations directly. The assumption usually made is that the fragments are in the same vertical plane as the shot line (the penetrator trajectory before impacting the target). Therefore, the scaling factor (K_v) that was evaluated to obtain the striking velocity is used to scale the coordinates.

II.2 MATCHING ORTHOGONAL FILM IMAGES AND CALCULATING FRAGMENT MASS

Before the spatial location of a specific fragment can be determined from the images in the orthogonal films, it is necessary to determine which image in each film was caused by that fragment. A pair of orthogonal images that can be assigned to an individual fragment is called a match. The procedure for matching images is based on the fact that both film planes share a common axis - the Z axis. Therefore, the extreme endpoints in the Z direction of the fragment in space appear as the extreme endpoints in the Z direction of the image on each orthogonal film. Maximum accuracy in evaluating the K factors (and, therefore, the spatial coordinates) occurs for those images where there is a unique Y value and a unique X value on the respective films to pair to each Z endpoint. When, for example, there are a range of Y values for an image in the vertical film that can be paired to a Z endpoint, the values calculated for the K factors will vary depending on what value is selected over the range of Y values but the values for the K factors will vary only slightly. The reason for this is that the magnitude of the change in the Y values is small compared to the head-to-film distance. For example, assuming that $Y_{hf}=X_{hf}=54$, $Y_{ff}=X_{ff}=8$, $X_1=7$ and $Y_1=7$, then $K_v=0.87341$. Allowing Y_1 to vary over a range of 1 (which represents an unusually large range) so that $Y_1=6$, then $K_v=0.89224$ or a change of about 2%. This would mean a possible 2% error in determining the spatial Z coordinate value.

The first step in the process for matching orthogonal images is the selection of the minimum Z endpoint of each pair of orthogonal images, computing the K factor for each endpoint and then scaling the Z values to the spatial coordinates by using Equations 9a and 9b. If these scaled Z values are

within some tolerance value (typically 10 mm) - to make allowance for slight errors in measuring the coordinate values - then the image endpoints were determined by the single spatial point located at the minimum Z coordinate value of the fragment. The next step is to process the maximum Z endpoints of the images in an identical manner. When both the minimum Z endpoints and the maximum Z endpoints are within the tolerance value, the matching process for this pair of images can be terminated if all of the film images are well separated. Usually, the images are not well separated, so two more steps are taken to make a final selection on which images will be declared a match.

The next step is to test to see if the sign of the difference between the two minimum Z endpoints is the same sign as the difference between the two maximum Z endpoints (when taken in the same order). This is based on the theory that the error in measuring the Z endpoints of each image will have the same sign - that is, be displaced in the same direction. This error can occur when the fiducial wires are shifted out of position when inserting the film cassette and are not returned to their normal position. This is manifested by the fiducial wire images not being perpendicular to each other.

The final step in the matching process is to select the pair of images for which the Z length of each image is most nearly alike. The Z length is the maximum Z endpoint minus the minimum Z endpoint where the Z endpoints are the values obtained from Equations 9a and 9b.

To summarize, the matching procedure is outlined as follows:

- (1) Select an image from the vertical film (List 1).
- (2) Select an image from the horizontal film (List 2).
- (3) Compute the K factors for the minimum Z endpoints of the two images.
- (4) Adjust the Z values using the appropriate K factor.
- (5) Take the absolute value of the difference between the two adjusted Z values.
- (6) If this difference is greater than the selected tolerance value (typically 10 mm.) then return to Step 2 selecting a new image from List 2 or if it is depleted then Step 1.

- (7) Repeat Steps 3 through 6 using the maximum Z endpoints.
- (8) For those that meet the tolerance test for both minimum and maximum endpoints, then test to see that the displacement between the two minimum Z points is in the same direction as the displacement in the two maximum endpoints. If not, then return to Step 2 or, if appropriate, Step 1.
- (9) More than one image may qualify as a match based on the above tests. The final match is determined by selecting the pair of images that are most nearly identical in Z length.

For each pair of matched images, an estimate of the volume of the fragment can be determined. Briefly, the volume is estimated by evaluating the area of the matched image in each orthogonal film, constructing a rectangle of equivalent area as that of the image and then scaling both rectangles to the spatial position of the fragment. This results in a rectangular parallelepiped representing the maximum possible volume of the fragment. Since this is the maximum possible volume, an empirically determined percentage of the volume is taken to represent the actual volume of the fragment.

The first step in determining the area of an image is to outline the image with a series of connected straight line segments as depicted in Figure 4. Then, proceeding in a clockwise direction around the boundary, the endpoints of the straight line segments are digitized (the coordinates of the endpoints are evaluated) and the values substituted in one of the following equations, depending on which film plane is being processed. This procedure is continued until the outline of the image has been traced back to the starting point.

$$A_{yz} = \frac{1}{2} \sum_{i=1}^N (Y_i Z_{i+1} - Y_{i+1} Z_i) \quad (12)$$

$$\text{or } A_{xz} = \frac{1}{2} \sum_{i=1}^N (X_i Z_{i+1} - X_{i+1} Z_i) \quad (13)$$

The centroid of the image is also evaluated since it is used to position the rectangle which will represent the image. The centroid for an image in the vertical film is calculated using the following equations:

$$Y_c = \frac{-1}{6A_{yz}} \sum_{i=1}^N (Z_{i+1} - Z_i)(Y_i^2 + Y_i Y_{i+1} + Y_{i+1}^2) \quad (14)$$

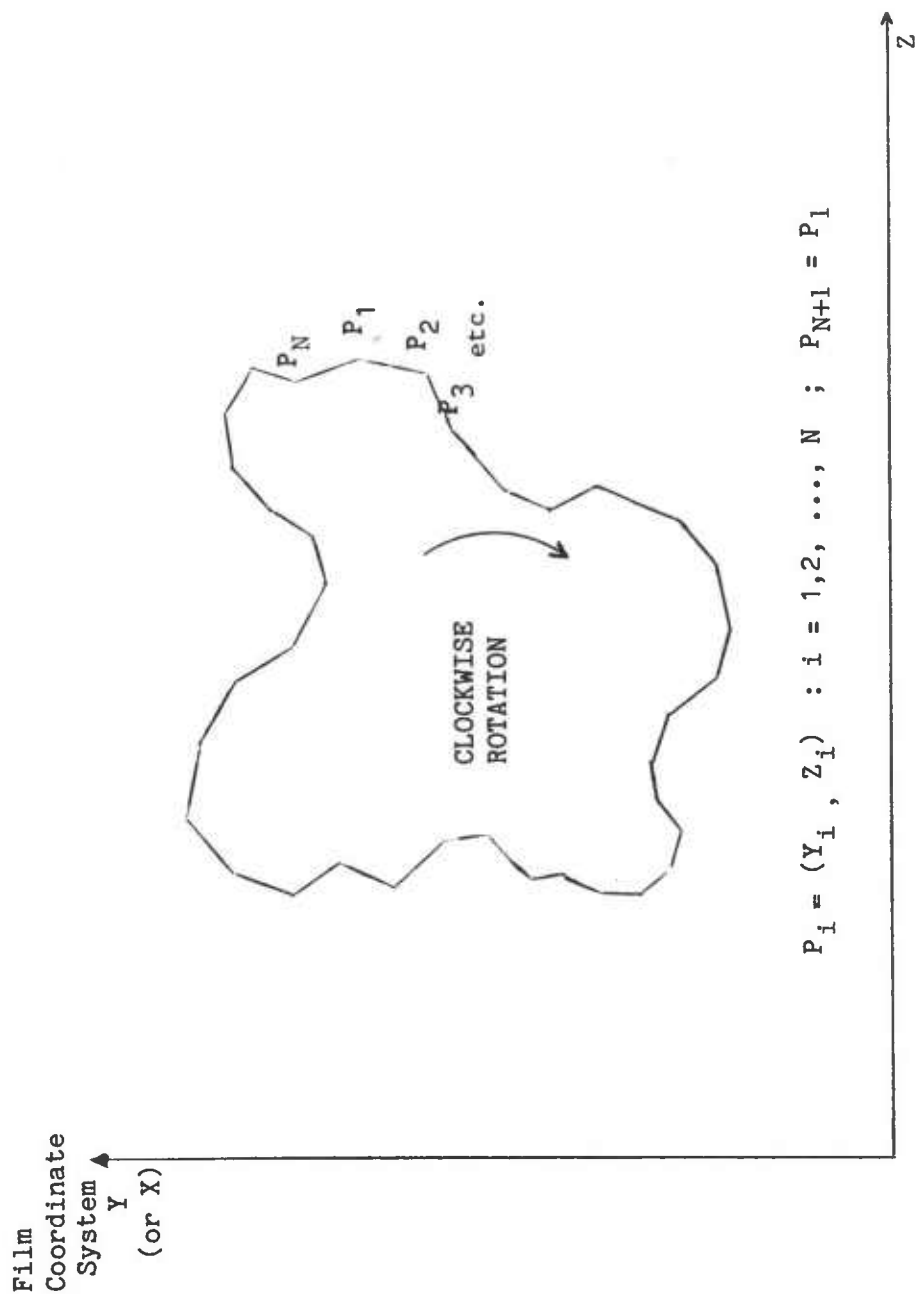


Figure 4 Representation Of The Image By Interconnecting Straight Line Segments

$$\text{and } Z_{cv} = \frac{1}{6A_{yz}} \sum_{i=1}^N (Y_{i+1} - Y_i)(Z_i^2 + Z_i Z_{i+1} + Z_{i+1}^2) . \quad (15)$$

The centroid for an image in the horizontal film is calculated using the following equations:

$$X_c = \frac{-1}{6A_{xz}} \sum_{i=1}^N (Z_{i+1} - Z_i)(X_i^2 + X_i X_{i+1} + X_{i+1}^2) \quad (16)$$

$$\text{and } Z_{ch} = \frac{1}{6A_{xz}} \sum_{i=1}^N (X_i - X_{i+1})(Z_i^2 + Z_i Z_{i+1} + Z_{i+1}^2) . \quad (17)$$

The signs involved in the equations for the centroid require a clockwise rotation as the boundary line segments are being traced. The summations involved in the centroid equations are evaluated at the same time that the summation for the area equation is computed. Upon returning to the starting point, the value for the area will have been determined and the calculations for the centroid can be completed. For Equations 12 - 17, the N+1 point is the same as the starting point.

The position of the sides of the rectangle which will represent the image is determined by aligning the sides with the Z endpoints. The "top" and "bottom" of the rectangle is determined by centering the rectangle in the Y (or X) direction on the centroid. This is illustrated in Figure 5. The location of the point to represent the "top" of the rectangle is chosen to be the point aligned "above" the Z coordinate of the centroid. Likewise, the point aligned "below" the Z coordinate of the centroid represents the "bottom" of the rectangle. The equations involved in establishing these points for the vertical film are the following:

$$\Delta Z = (Z_{\max} - Z_{\min}) , \quad (18)$$

$$\Delta Y = A_{yz} / \Delta Z , \quad (19)$$

$$\text{"top" point} = (Y_{cv} + \Delta Y/2, Z_{cv}) \quad (20)$$

$$\text{and the "bottom" point} = (Y_{cv} - \Delta Y/2, Z_{cv}) . \quad (21)$$

Similar equations apply for the image in the horizontal film.

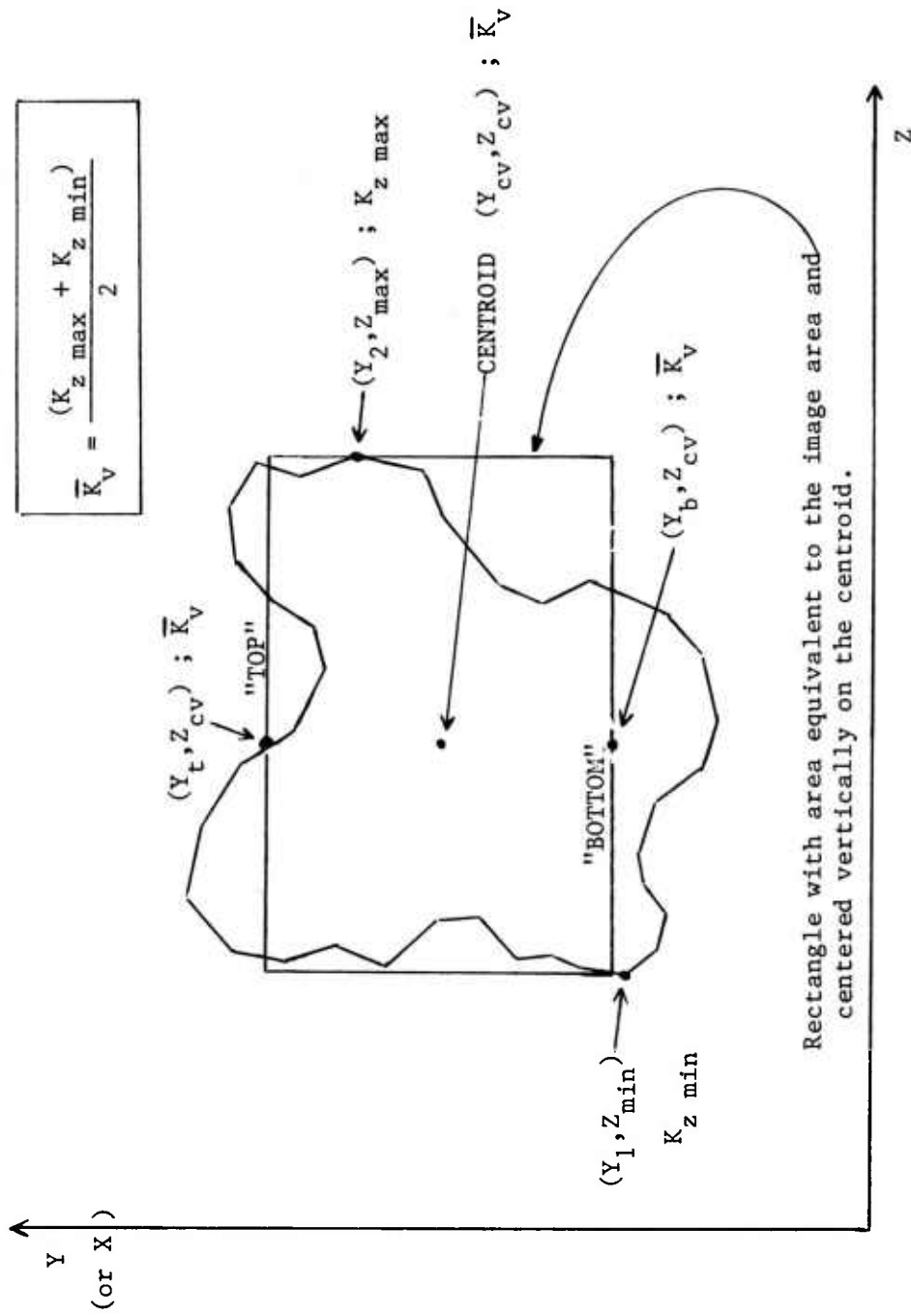


Figure 5 Representing The Image By A Rectangle Of Equivalent Area And Indicating The K Factor Associated With Each Point.

To summarize, there are five points associated with each film image. These five are the minimum Z end point, the maximum Z endpoint, the centroid, the "top center" point and the "bottom center" point. For each pair of matched images, the five points from each image are scaled using Equation 9a, 9b, 10 or 11 appropriately to form a rectangular parallelepiped in the spatial coordinate system. (The K factor which is used to scale the "top" point, the centroid and the "bottom" point is the average value of the K factors for the Z endpoints.) The parallelepiped represents the maximum possible volume of the fragment. To represent the actual volume of the fragment, a fractional part of volume of the rectangular parallelepiped is required. A satisfactory value for this percentage value will be determined in the next subsection.

Once the volume of the fragment has been calculated, the mass is computed by multiplying the volume by the density of the fragment. (If the target and penetrator are made from different materials, it may be necessary to guess which density should be used.) The equation to compute the mass of the fragment is:

$$M_f = q \rho_f \Delta X' \Delta Y' \Delta Z' . \quad (22)$$

where: q is the fractional volume value, ρ_f is the fragment density and the primes indicate that the dimensions of the rectangular parallelepiped are determined from the scaled coordinate points (i.e., the spatial coordinate points).

II.3 A TEST OF THE METHODOLOGY FOR MATCHING IMAGES AND THE DETERMINATION OF THE FRACTIONAL VALUE q

To demonstrate how well the methodology for matching images works, six irregular shaped fragments ranging in mass from 9.75 grams to 148.5 grams were selected from an assortment of fragments recovered from a firing range. These fragments were mounted at various positions on a piece of styrofoam in such a way that the projected images on the each of the orthogonal films would be completely separated from each other. A pair of orthogonal X-ray tubes were pulsed and the resulting images formed on the two orthogonal films were analyzed using the procedure described in the previous subsection. The measured Z endpoints and the calculated coordinates ("top," centroid and "bottom") representing the rectangle with an equivalent area to that of each image on the film are tabulated in Tables 1 and 2 along with the computed areas of the images on the film. Table 3 shows the results of matching the images. Since the images were well separated, a unique match was found for each of the images.

TABLE 1 VERTICAL FILM COORDINATE VALUES FOR A TEST CASE*

IMAGE #	LEFT		CENTROID		RIGHT		"TOP"		"BOTTOM"		AREA (sq cm)
	Y	Z	Y	Z	Y	Z	Y	Z	Y	Z	
	(cm)	(cm)	(cm)	(cm)	(cm)	(cm)	(cm)	(cm)	(cm)	(cm)	
1	25.43	-9.02	25.81	-8.15	25.68	-7.44	26.26	-8.15	25.35	-8.15	1.4290
2	25.86	-5.82	25.78	-3.02	27.94	-0.51	27.41	-3.02	24.13	-3.02	17.4393
3	21.06	-4.37	19.28	-2.97	17.17	-1.65	21.23	-2.97	17.35	-2.97	10.5980
4	8.69	3.53	8.64	5.16	9.32	6.63	10.13	5.16	7.11	5.16	9.4303
5	23.95	10.62	23.98	11.91	24.16	13.26	25.48	11.91	22.48	11.91	7.9039
6	29.21	7.85	29.57	10.92	28.93	15.14	30.68	10.92	28.45	10.92	16.2045

* Case identified as # STAT-82-01-13-2.

TABLE 2 HORIZONTAL FILM COORDINATE VALUES FOR A TEST CASE*

IMAGE #	LEFT		CENTROID		RIGHT		"TOP"		"BOTTOM"		AREA (sq cm)
	X (cm)	Z (cm)	X (cm)	Z (cm)	X (cm)	Z (cm)	X (cm)	Z (cm)	X (cm)	Z (cm)	
1	14.81	-4.50	14.22	-3.15	14.40	-1.65	14.78	-3.15	13.67	-3.15	3.1658
2	24.97	-9.02	25.02	-8.20	24.51	-7.39	26.47	-8.20	23.57	-8.20	4.6871
3	26.21	-5.69	26.59	-2.92	25.91	-0.38	27.89	-2.92	25.27	-2.92	13.8942
4	18.75	3.30	21.18	4.75	22.66	6.12	24.87	4.75	17.50	4.75	20.7354
5	13.54	11.48	14.22	12.78	14.07	14.30	14.76	12.78	13.69	12.78	3.0445
6	24.59	8.26	23.72	11.33	24.26	15.80	26.19	11.33	21.23	11.33	37.3812

* Case identified as # STAT-82-01-13-2

TABLE 3 MATCHED IMAGE PAIRS (SCALED SYSTEM COORDINATES) FOR A TEST CASE*

VIEW	IMAGE #	LEFT			CENTROID			RIGHT			$\Delta X'$ (cm)	$\Delta Y'$ (cm)	$\Delta Z'$ (cm)
		X or Y (cm)	Z (cm)		X or Y (cm)	Z (cm)		X or Y (cm)	Z (cm)				
Vert.	3	20.98	-3.89		19.41	-2.64		17.53	-1.47				
Horiz.	1	15.67	-3.81		15.09	-2.69		15.16	-1.45		0.955	3.454	2.388
Vert.	1	24.51	-7.42		24.84	-6.73		24.74	-6.15				
Horiz.	2	24.13	-7.39		24.18	-6.73		23.75	-6.07		2.385	0.747	1.295
Vert.	2	24.84	-4.75		24.79	-2.46		26.54	-0.43				
Horiz.	3	25.14	-4.67		25.43	-2.39		24.82	-0.30		2.126	2.690	4.343
Vert.	4	10.29	3.05		10.39	4.37		11.13	5.54				
Horiz.	4	18.87	3.05		21.11	4.37		22.48	5.61		6.802	2.573	2.527
Vert.	5	23.57	9.47		23.57	10.62		23.72	11.79				
Horiz.	5	14.71	9.50		15.29	10.57		15.16	11.81		0.892	2.654	2.311
Vert.	6	27.69	6.48		27.97	9.04		27.46	12.55				
Horiz.	6	23.72	6.60		23.04	9.04		23.47	12.65		3.962	1.839	6.058

* Case identified as # STAT-82-01-13-2

The maximum possible mass for each matched image pair, found by multiplying the density of steel (7.78 g/cc) by the volume of the rectangular parallelepiped, is tabulated in the fifth column of Table 4. The ratio of the measured mass to the calculated mass is tabulated in the sixth column of Table 4. The average value of these ratios is 0.47. Therefore, it is suggested that the mass of an irregular shaped fragment can be estimated from the following equation.

$$M_f = 0.47 \rho_f \Delta X' \Delta Y' \Delta Z' . \quad (23)$$

The percentage error in calculating the mass using this equation ranges from 3.6% to 17.7% for these six fragments. The average error is 11.4%.

II.4 ESTIMATING FRAGMENT VELOCITY BASED ON ORTHOGONAL FILM IMAGES

Calculating the velocity of a fragment requires establishing the position of the fragment at two locations and the time interval which elapsed while the fragment travelled from the first location to the second. Two methods for calculating fragment velocity will be described.

The first method requires only one X-ray station (one set of orthogonal X-ray tubes) and makes use of two simplifying assumptions. The first assumption is that all fragments leave from a single point and the second assumption is that they all leave from that point simultaneously. The following discussion concerning the magnitude of the error involved by making these assumptions will be based on the situation where fragments leave the rear surface of the target as a result of complete penetration.

The magnitude of the error involved in making the first assumption (fragments leaving from a single point) is small since the dimensions of the exit hole are small compared to the distance the fragments have travelled by the time the X-ray tubes are flashed. This single point is chosen to be the center of the exit hole in the original plane of the rear surface of the target. It is denoted by the coordinates X_e , Y_e , Z_e where the reference origin is the same as that of the film and spatial coordinate system.

TABLE 4 CALCULATED MASS FROM FLASH RADIOGRAPHS FOR A TEST CASE*

HORIZONTAL IMAGE #	VERTICAL IMAGE #	FRAGMENT ID #	MASS (grams)		RATIO MEAS./CALC.	CALC. EQ. 23	PERCENTAGE ERROR
			MEASURED	CALC. MAX.			
1	3	8	27.80	61.28	0.454	28.8	3.6
2	1	13	9.75	17.95	0.543	8.4	-16.1
3	2	4	82.70	193.23	0.428	90.8	8.9
4	4	2	142.70	344.08	0.415	161.7	13.3
5	5	10	24.30	42.56	0.571	20.0	-17.7
6	6	1	148.50	343.40	0.432	161.4	8.7
			AVERAGE		0.474		11.4

* Case identified as # STAT-82-01-13-2

The magnitude of the error involved in making the second assumption is more difficult to ascertain. It is thought that the period of time required for the fragments to reach their maximum velocity is small compared to the interval of time culminating in the flash of the X-ray tubes.

The magnitude of the total error is dependent on the method used to establish the beginning of the time interval to be used in the velocity calculation. The recommended method for establishing the beginning of the time interval is to place a trigger break screen approximately one inch (2.54 cm) behind the target parallel to the rear surface by using a layer of flexible foam material. The time interval used in the velocity calculation is the time between the instant the screen is broken (which triggers a time counter) to the instant the X-ray tubes are pulsed (stopping the time counter). This time interval will be denoted as Δt in the equation below.

Using this method, the equation for calculating the velocity of fragments which have been identified by matched image pairs is:

$$v_f = \frac{\sqrt{(x_p - x_e)^2 + (y_p - y_e)^2 + ((z_{ph} + z_{pv})/2 - z_e)^2}}{\Delta t} \quad (24)$$

where x_p , z_{ph} and y_p , z_{pv} are the scaled coordinates (spatial coordinates) of the centroids.

The second method for computing fragment velocities requires two orthogonal X-ray stations (a pair of orthogonal X-ray tubes at each station) behind the target. Since the same film is exposed by the flash from each X-ray station, the images of the fragments produced by the flash from the first X-ray station lie close to the images produced by the flash from the second X-ray station. It is frequently difficult to determine to which station each image should be assigned. (This problem will not arise in the ADAS because the images from each X-ray station will be separate from those of any other station.)

The orthogonal images are matched at each station in the manner described in the previous subsection. Then the images at one station must be matched to the images at the other station. This is not easy to do since the image of a fragment at one station does not necessarily look the same as its related image at the subsequent station due to rotation and tumbling. One way to make the match is to determine the trajectory of a fragment at the first station based on a virtual reference point (one point for all the fragments) and look for a fragment at the second station which lies on that trajectory. When a

match can be made, the velocity can be determined by evaluating Equation 24 with X_e, Y_e, Z_e replaced by the coordinates of the centroid of the fragment at the first station and using the time interval between station flashes for Δt .

For those images where a match can be made at each station and between stations, this method is more accurate than the first. However, it is more difficult to implement and takes a much longer time to evaluate since more calculations are involved.

III. AUTOMATING THE FILM DIGITIZATION PROCESS

The paramount shortcoming in the analysis of film is the tedious work which still must be performed by hand. The person analyzing the film becomes fatigued after a short period of time so that many of the images are ignored and mistakes are more readily made. Consequently, an automatic technique for performing the digitization would lead to a savings in time for the analyst and a substantial improvement in accuracy.

A proposed method for automating the film digitization process is based on utilizing a video camera to scan the film in a systematic fashion. Because the angular camera view is restricted, a mechanical device is required which can move the film so that adjacent sections of the film are positioned into the field of view of the camera in a known sequence. Preferably, the film sections do not overlap and all of the film is processed. The video camera records the light intensity level (gray level) of the backlighted film which is digitized using an analog to digital (A/D) converter. The digitized signal is then transferred to a computer for analysis.

The software (computer program) for controlling the analysis should include a routine which will determine which dots (pixels) are to be associated with each image. For each image which is resolved, the area and the five points describing the image are determined analogous to the method described in Section II. Incorporated in the software package should be the software which has already been developed for determining the fragment mass and the velocity.

This method of analyzing the X-ray film has an added benefit. Since the equipment that processes the signal from the video camera is recording intensity levels (gray levels), the variation in the intensity is a measure of how much metal attenuated the X-ray radiation from the pulsed tubes. That is, the thicker the fragment, the more X-rays are blocked and the image on the film

reflects that attenuation. Therefore, the mass can be estimated directly.^{3,4}

IV. THE AUTOMATIC DATA ACQUISITION SYSTEM (ADAS)

A block diagram of the ADAS is shown in Figure 6. The X-ray side of the system (the X-ray tubes) is the same as current conventional range setups. The tubes are pulsed using the same triggering mechanism as now and with the same equipment. What is different from the conventional setup is that the film has been replaced by a set of video cameras. The intensifier screens (also used with the conventional film system), which are located in front of the cameras, convert the X-ray radiation that impinges on the screen to visible light. The images of the fragments appear as dark areas on the intensifier screen since the fragments attenuate or block the radiation. A lens focuses the view of the intensifier screen onto the photo-cathode of a micro-channel plate (MCP) image intensifier tube when the MCP is turned on (triggered by the same pulse that triggered the associated X-ray tube) by the operation of a control unit. In addition to acting as a shutter, the MCP amplifies the light focused on its photo-cathode. The gain of the MCP amplifier is approximately 1000 which is sufficient to compensate for the extremely short exposure time that the MCP is gated on. (The exposure time is comparable in length to the duration of the X-ray pulse of radiation which is approximately 70 nanoseconds and precludes blurred images of the fragments.) The amplified light signal is coupled through a fiber optic cable to the vidicon tube of the video camera.

Figure 7 is a schematic representation of a vidicon camera tube. The signal electrode is operated at a positive voltage with respect to the photo-conductive target (PCT) which operates at the cathode (near zero) voltage. Before the MCP has been gated on, the back side of the PCT is charged by the action of a scanning electron beam which is supervised by the control unit. When the MCP is gated on, the scanning electron beam is blanked off and the light pattern projected by the optic fiber cable onto the PCT causes its conductivity to increase in the illuminated areas. This increased conductivity causes the adjacent areas on the rear of the PCT to charge to more positive values. The MCP is then gated off so that X-ray radiation from any tubes that

⁵ Haskell, Donald F., "Intensity Integration of Flash Radiograph Images," *Proceedings of the Third Annual Vulnerability Survivability Symposium*, Naval Amphibious Base, Coronado, San Diego, CA, 8-10 Nov 77.

⁴ Fugelso, Erik, "Material Density Measurements From Dynamic Flash X-Ray Radiographs Using Axisymmetric Tomography," LA-8785-M, Los Alamos Scientific Laboratory, Post Office Box 1663, Los Alamos, NM 87545.

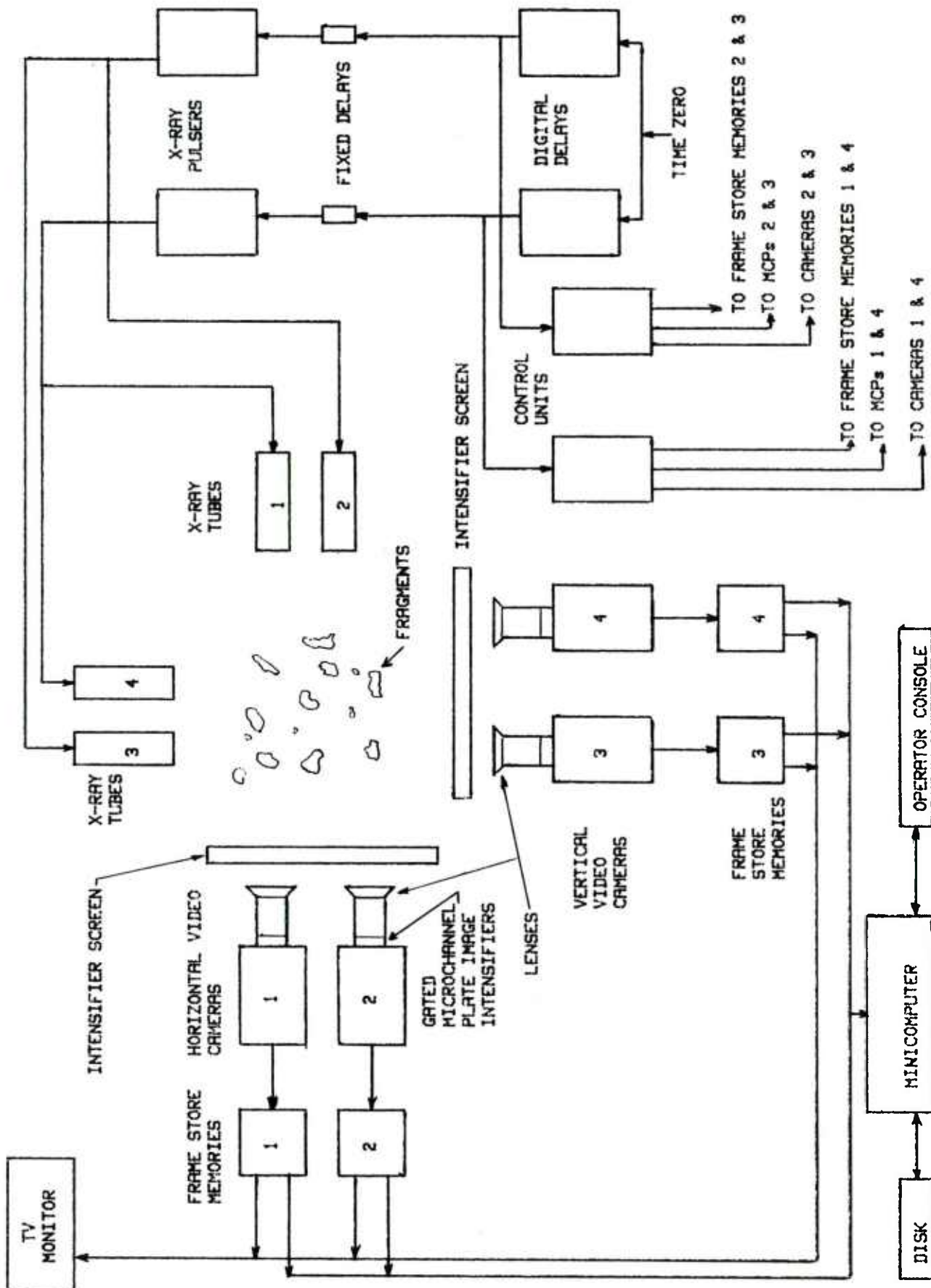


Figure 6 Block Diagram Of The ADAS.

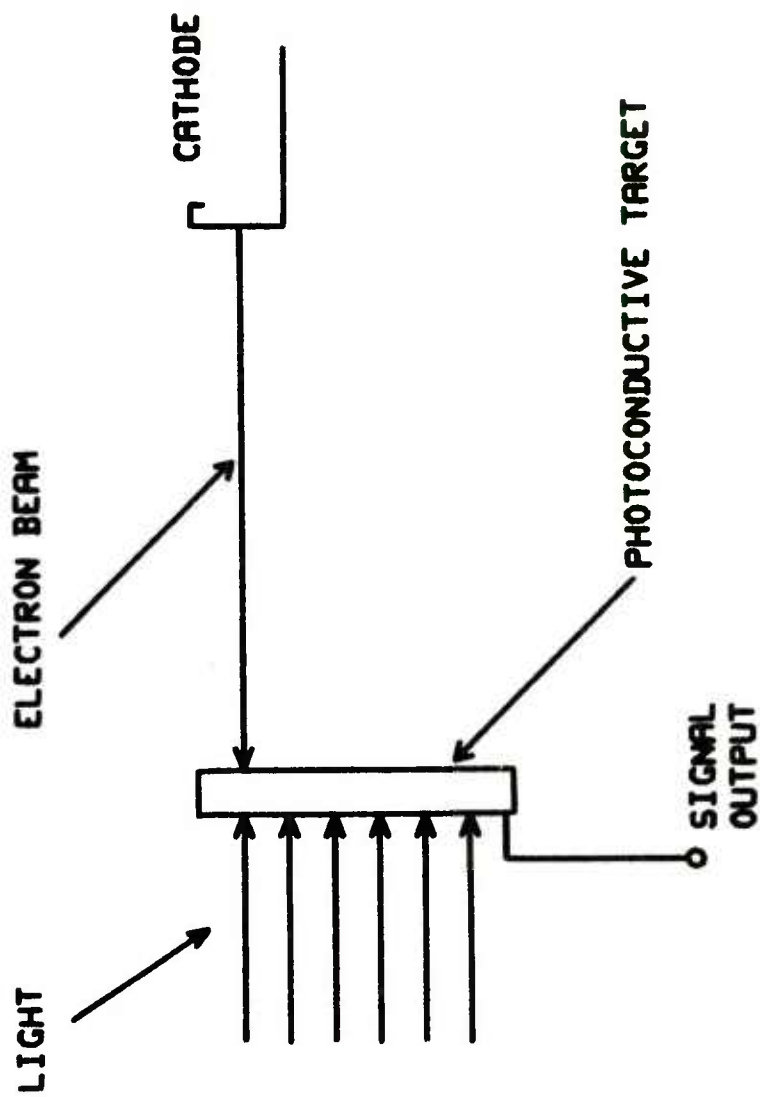


Figure 7 Schematic Representation Of A Vidicon Tube.

are subsequently pulsed will not affect the image pattern stored on the PCT. To process the image pattern, the scanning electron beam is turned on. The signal resulting from the electron beam interacting with the positively charged areas of the PCT is capacitively coupled to the signal electrode (designated signal output in Figure 7). This signal after amplification is the output signal from the video camera.

The output signal from the video camera is coupled to the A/D converter. The A/D converter periodically samples the output signal from the video camera and converts the amplitude of the signal at that instant to a digital value. This value corresponds to the intensity of the light at that position in the image pattern on the PCT. This action continues until two complete scans (one frame for standard interlaced video) of the PCT have taken place. The digitized signals are stored in contiguous memory locations of the frame store memories (see Figure 6) as one frame. The memory can then be dumped under control of the minicomputer to a mass storage device such as magnetic disk for "permanent" storage. The contents of each frame stored in memory can also be transferred to a digital to analog (D/A) converter which will reconstruct the image pattern that appeared on the MCP. The output of the D/A converter can be displayed on a video monitor permitting visual examination of the fragment image pattern.

The digitized data contained in the frame store memories (or on disk) recorded by each video camera can be analyzed using the methods described in Section II and III. Since the image pattern in each frame represents a single "snapshot" of the action and since the data is already in the correct form to be used by a computer, the analysis will be much easier than that required when film is used to record the fragment images.

The resolution of the ADAS is limited primarily by the MCP image intensifier tube. It is also dependent on the size of the area to be viewed. For a 500 x 500 millimeter viewing area, the resolution should be about 1 mm at the bright parts of the image. Technological advances will likely improve the resolution. If the resolution is not deemed adequate, two advantages to the ADAS should be taken into consideration. The first advantage is that the image data is handled entirely electronically, thereby eliminating human error. The second advantage is that single "snapshot" views of the action are obtained - eliminating errors due to overlapping image regions which are often a problem with multiframe sequences on flash radiographs.

V. SUMMARY AND CONCLUSIONS

This report presents three different levels of analytic techniques for determining mass and velocity of dynamic fragments (fragments in motion). The first level describes recent advancements for analyzing images on flash radiographs. This advancement has reduced the amount of physical labor and inaccuracies but the procedure can still be made less tedious by introducing the system which constitutes the second level. This second level consists of a proposed technique for eliminating the need to digitize the film manually. This advancement is entirely feasible but requires the procurement of some hardware and the development of some computer software for the necessary manipulation of the digitized data. The third level is the development of the ADAS which is the ultimate in automatic recording of dynamic fragment images. This system will minimize the tedious handwork for the analyst and will significantly increase the accuracy of the results. The implementation of the ADAS will require procurement of hardware and the development of additional computer software. The installation of the video cameras will require modifications to existing firing ranges since the cameras will require more space than the film cassettes. It may be found that the ADAS will be useful for studying other physical phenomena such as shaped charge jet and self-forging fragment formation.

ACKNOWLEDGEMENTS

The authors thank Mr. John Polk of the Terminal Ballistics Division (TBD) for providing the equations for computing the area and the centroid of a closed figure bounded by connecting straight line segments and Mr. Bill Wright, also of the TBD, for encouragement and assistance in preparing this report.

DISTRIBUTION LIST

<u>No. of</u> <u>Copies</u>	<u>Organization</u>	<u>No. Of</u> <u>Copies</u>	<u>Organization</u>
2	Commander Defense Technical Info Center ATTN: DTIC-DDA Cameron Station Alexandria VA 22314	1	Commander US Army Communications Rsch. and Development Command ATTN: DRSEL-ATDD Fort Monmouth NJ 07703
1	Commander US Army Materiel Development and Readiness Command ATTN: DRCMD-ST 5001 Eisenhower Avenue Alexandria VA 22333	1	Commander US Army Electronics Research and Development Command Technical Support Activity ATTN: DELSD-L Fort Monmouth NJ 07703
1	Commander US Army Armament Research and Development Command ATTN: DRDAR-TDC Dover NJ 07801	1	Commander US Army Missile Command ATTN: DRSMI-R Redstone Arsenal AL 35898
2	Commander US Army Armament Research and Development Command ATTN: DRDAR-TSS Dover NJ 07801	1	Commander US Army Missile Command ATTN: DRSMI-YDL Redstone Arsenal AL 35898
1	Commander US Army Armament Materiel Readiness Command ATTN: DRSAR-LEP-L Rock Island IL 61299	1	Commander US Army Tank Automotive Command ATTN: DRSTA-TSL Warren MI 48090
1	Director US Army Armament Research and Development Command Benet Weapons Laboratory ATTN: DRDAR-LCB-TL Watervliet NY 12189	1	Director US Army TRADOC Systems Analysis Activity ATTN: ATAA-SL White Sands Missile Range NM 88002
1	Commander US Army Aviation Research and Development Command ATTN: DRDAV-E 4300 Goodfellow Blvd. St. Louis MO 63120	2	Commandant US Army Infantry School ATTN: ATSH-CD-CSO-OR Fort Benning GA 31905

DISTRIBUTION LIST (continued)

<u>No. of</u> <u>Copies</u>	<u>Organization</u>	<u>No. Of</u> <u>Copies</u>	<u>Organization</u>
1	Director US Army Air Mobility Research and Development Laboratory Ames Research Center Moffett Field CA 94035		<u>Aberdeen Proving Ground</u> Dir, USAMSAA ATTN: DRXSY-D DRXSY-MP, H. Cohen Cdr, USATECOM ATTN: DRSTE-TO-F Director,USACSL, BLDG E3516, EA ATTN: DRDAR-CLB-PA DRDAR-CLN DRDAR-CLJ-L
1	AFWL/SUL Kirtland AFB, NM 87117		

USER EVALUATION OF REPORT

Please take a few minutes to answer the questions below; tear out this sheet, fold as indicated, staple or tape closed, and place in the mail. Your comments will provide us with information for improving future reports.

1. BRL Report Number _____
2. Does this report satisfy a need? (Comment on purpose, related project, or other area of interest for which report will be used.)

3. How, specifically, is the report being used? (Information source, design data or procedure, management procedure, source of ideas, etc.) _____

4. Has the information in this report led to any quantitative savings as far as man-hours/contract dollars saved, operating costs avoided, efficiencies achieved, etc.? If so, please elaborate.

5. General Comments (Indicate what you think should be changed to make this report and future reports of this type more responsive to your needs, more usable, improve readability, etc.) _____

6. If you would like to be contacted by the personnel who prepared this report to raise specific questions or discuss the topic, please fill in the following information.

Name: _____

Telephone Number: _____

Organization Address: _____

